P-stop isolation study of irradiated n-in-p type silicon strip sensors for harsh radiation environment

Martin Printz on behalf of the CMS Tracker Collaboration

HSTD-10 Xi‘an China, Sept. 25th-29th, 2015

Institut für Experimentelle Kernphysik, KIT Germany

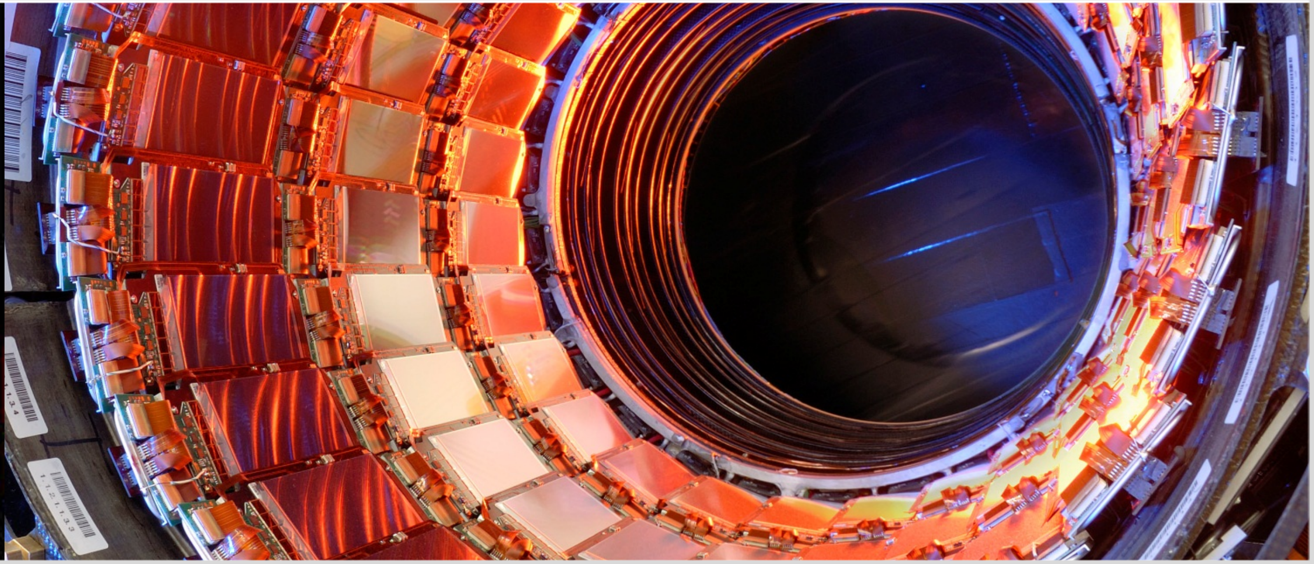

Outline

Position sensitive detectors
- The CMS Tracker

P-isolation
- N-in-p technology

Motivation
- R&D studies
- Observation of ghost hits in dependence of the p-isolation characteristics
- Search for possible new vendors

Results
- Interstrip resistance before and after irradiation
- Charge collection studies
- Electric field strength

The current CMS Tracker

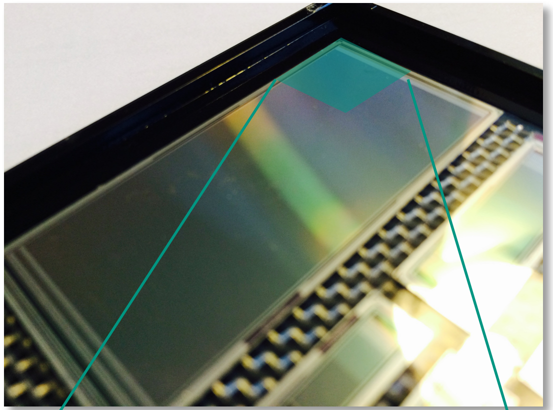

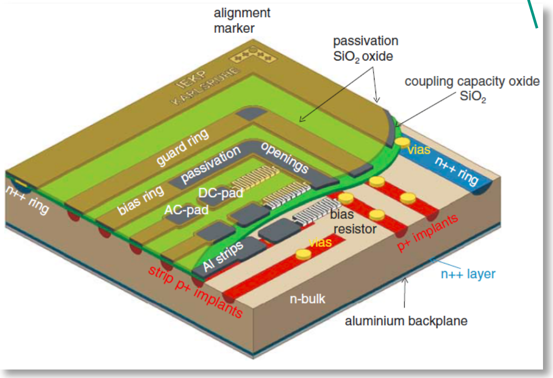

Fig.: Schematic of a strip detector

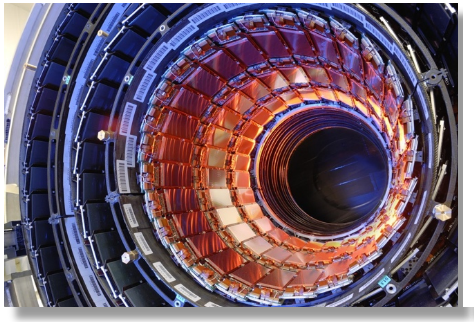

Fig.: CMS silicon tracker inner barrel (TIB)

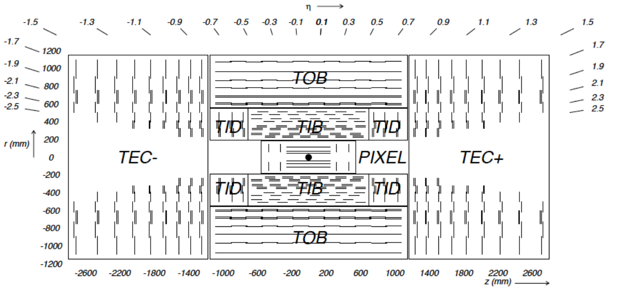

Fig.: CMS full tracker layout

- Dimension: 5.8 m x 2.5 m
- ~210 m^2 of silicon detectors (pixel & strips)
- Barrel and Endcaps cover the range of $\eta = -\ln\tan\left(\frac{\Phi}{2}\right)$ up to $|\eta| < 2.5$
- P-in-n and n-in-n technology
- Position measurement with up to 10 μm precision

- Will be fully exchanged during the LS3 ~2023
  - New tracker layout
  - Outer Tracker will be equipped with n-in-p type technology

CMS Tracker after Phase II Upgrade

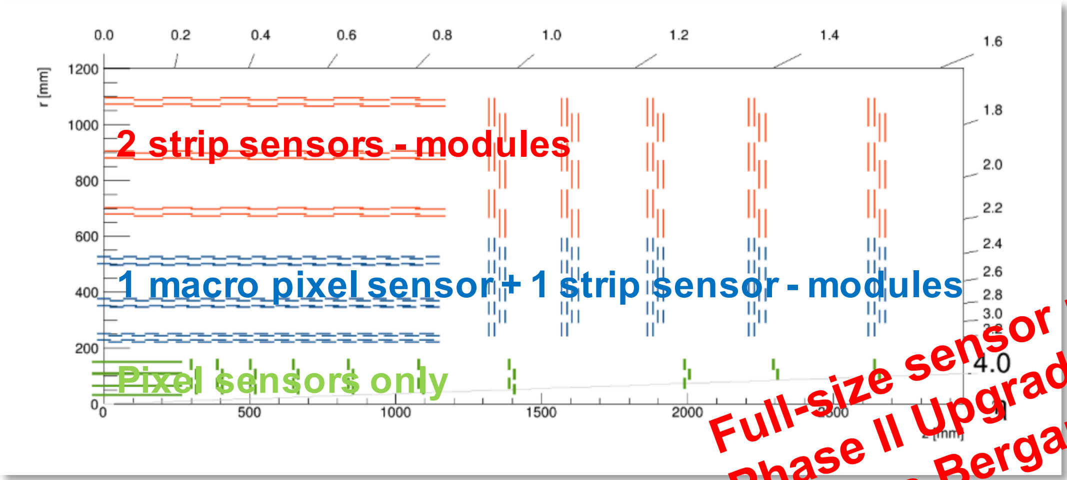

Full-size sensor prototypes for the
Phase II Upgrade of the CMS Tracker
Thomas Bergauer (see later this day)

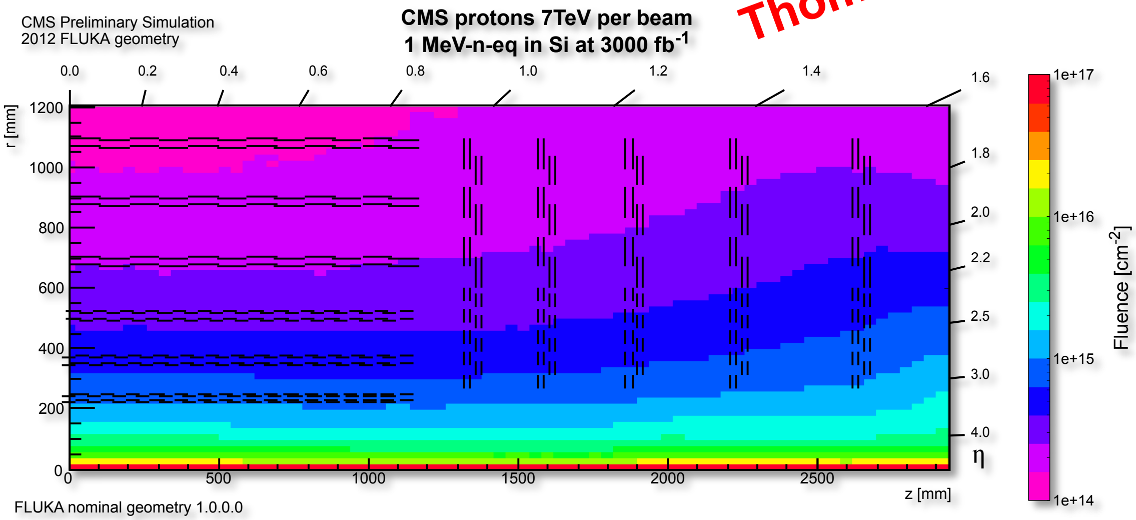
CMS Preliminary Simulation
2012 FLUKA geometry

CMS protons 7TeV per beam
1 MeV-n-eq in Si at 3000 fb^{-1}

FLUKA nominal geometry 1.0.0.0

- Sensors for 2S and PS modules will be n-in-p type technology

- Expected fluence after 3000fb^{-1} during the Phase II run for the Outer Tracker : **$1x10^{15}$ $n_{eq}cm^{-2}$**

- **Following results cover the fluence up to $2x10^{15}$ $n_{eq}cm^{-2}$**

CMS Tracker after Phase II Upgrade

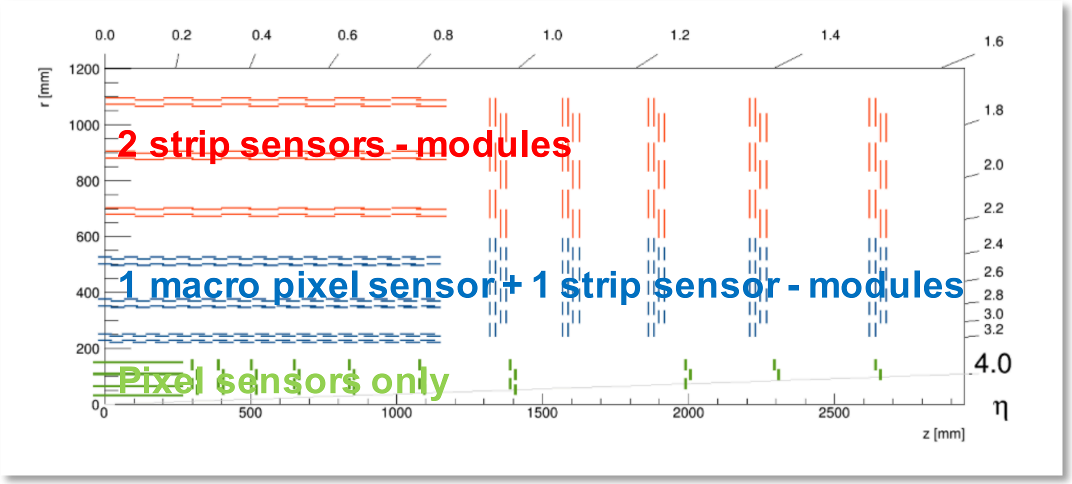

- Sensors for 2S and PS modules will be of n-in-p type technology

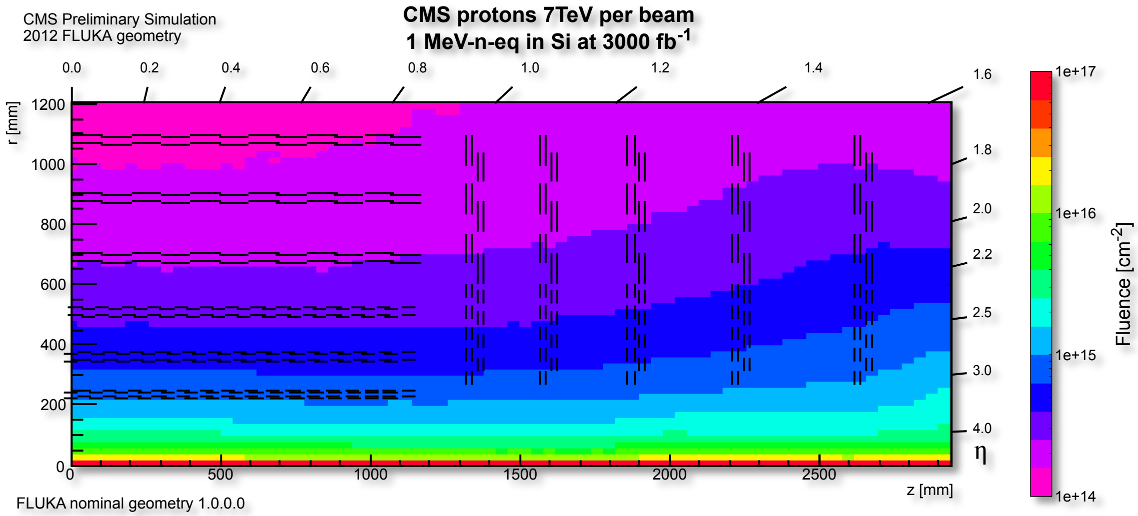

- Expected fluence after 3000 fb^{-1} during the Phase II run for the Outer Tracker : **1×10^{15} $n_{eq}cm^{-2}$**

- **Following results cover the fluence up to 2×10^{15} $n_{eq}cm^{-2}$**

N-in-p technology

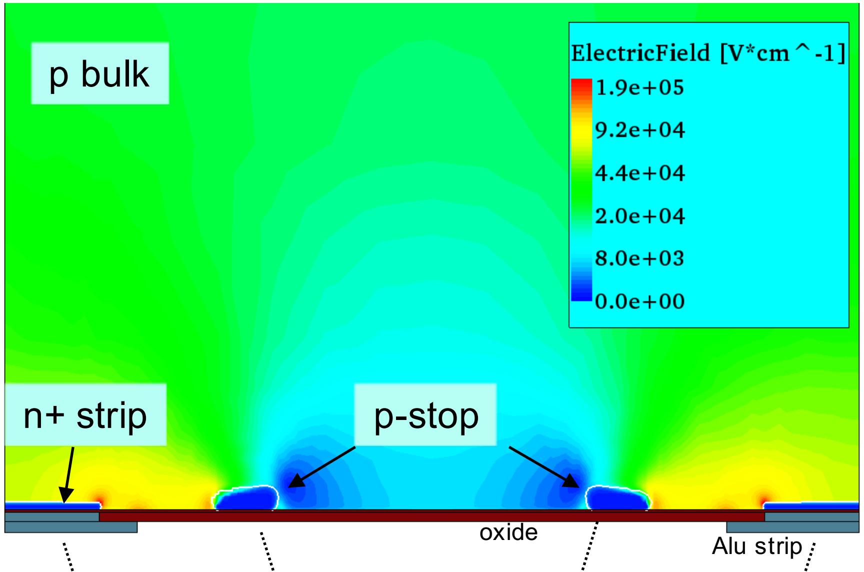

Different p+ process characteristics

- Prevent electron accumulation by p+ implantation between adjacent strips
- Isolation & strength of electric fields depend on p+
    - doping concentration
    - doping energy
    - doping depth

Different p-stop pattern:

- Distance between strip and p-stop

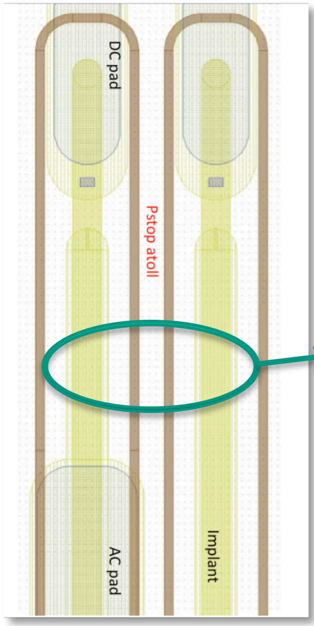

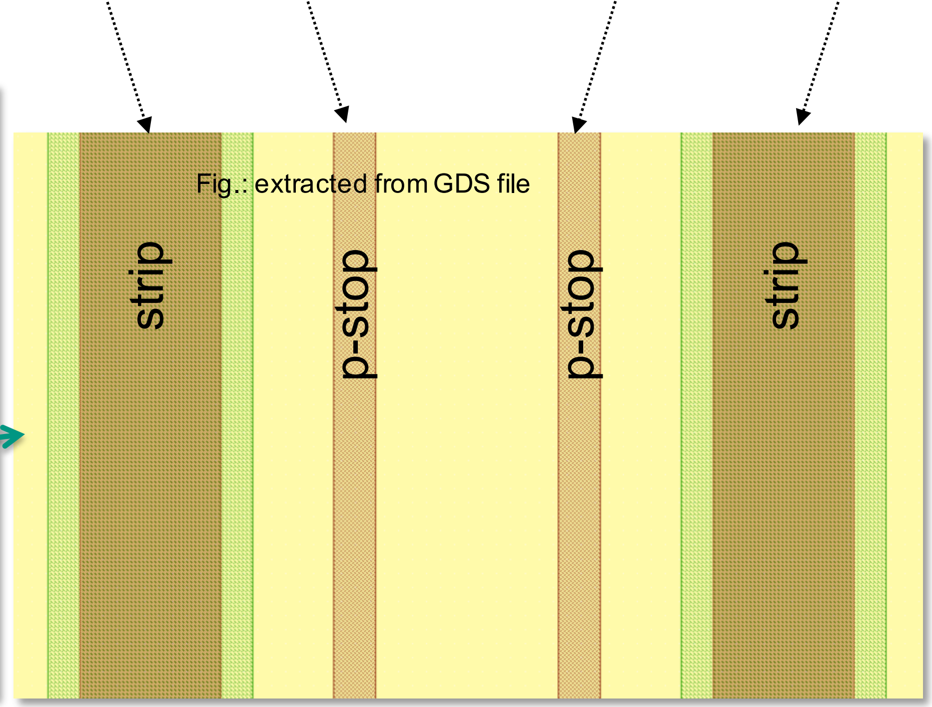

Fig.: extracted from GDS file

R&D studies:

- Neutrons + 23 MeV protons up to $\Phi=2\times10^{15}$ 1MeV n_{eq}/cm^2
- (X-ray studies: surface damage)
- T-CAD simulation

Interstrip resistance R_{int}

- N-in-p type sensor performance dependent on isolation characteristics
- Isolation technique affects noise and breakdown behaviour -> known from measurements and T-CAD studies
- Task: find the most suitable p+ isolation doping concentration and depth
  - lower maximum electric fields -> high breakdown voltage
  - ensure sufficient R_{int} -> low charge sharing despite of fluence

- **Approach: sensors with 5 different initial doping concentrations and depths (variants V)**

Variant #1	V #2	V #3	V #4
p-stop conc. ~ 1-5x10^{16} cm^{-3}	p-stop conc. ~ 9x10^{16} cm^{-3}	p-stop conc. << 1x10^{16} cm^{-3}	p-stop conc. ~1x10^{16} cm^{-3}
doping depth ~2.2 µm	doping depth ~2.7 µm	doping depth <2.0um	p-stop conc. ~1x10^{17} cm^{-3}
			doping depth ~1.5 µm
			doping depth ~2.5 µm

R&D studies: irradiation with protons, neutrons and x-rays
Electrical qualification, Sr90 measurements, telescope runs

Specifications for the productions

- Substrate material
  - Wafer size: 6" & 4"
  - Wafer type: p-type FZ
  - Crystal Orientation: <100>
  - Resistivity: 4 kΩcm – 10 kΩcm
  - Oxygen concentration: $< 2\times10^{16}$ cm^{-3}
  - Physical thickness: 200 μm – 300 μm
  - Strip pitch: 90 μm
  - Strip width: 25 μm

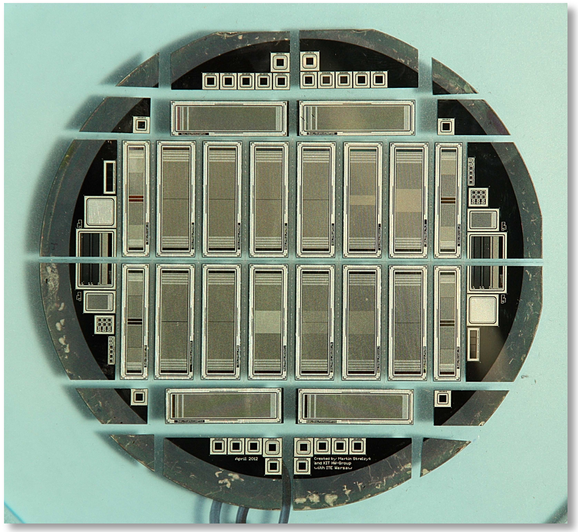

- Process details:
  - AC coupled with polysilicon bias or punch through and p-stop strip isolation
  - Definition of doping profiles
    - Peak doping concentration is defined as the maximum concentration slightly below the bulk surface
    - Full depth is defined as the depth below the bulk surface where the doping concentration has reached the bulk concentration

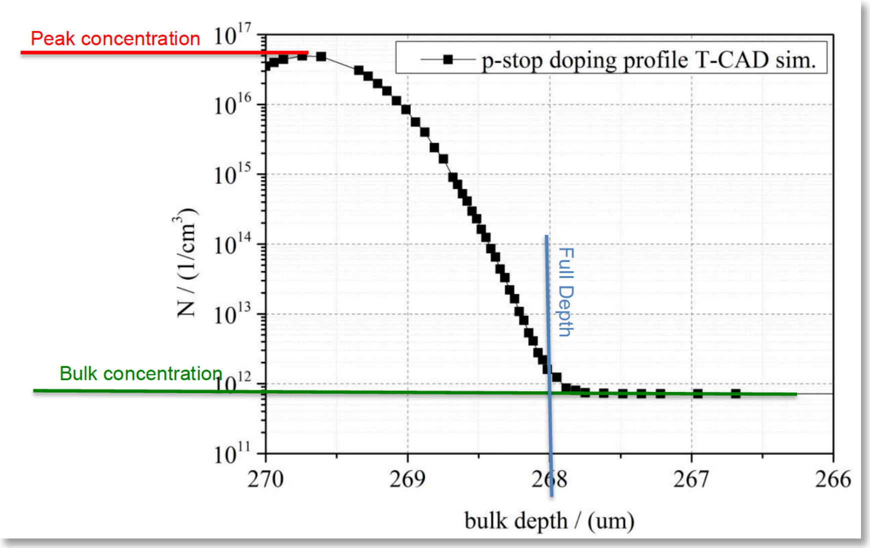

R_{int} - measurement

- *probestation* for electrical qualification of sensors
- R_{int} measurement
  - ramp to +1V between two adjacent strips (DC)
  - measure $1V/(I_{max}-I_{min})$
  - measurement of lower limit of R_{int}

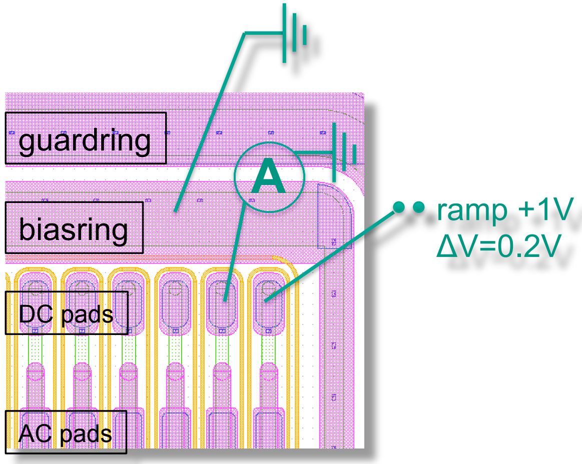

Results from the last huge R&D campaign

- R_{int} drops with fluence from several GΩcm to some 100MΩcm
- In this specific campaign (with no variations of p-stop conc.):
  - No dependence on technology (n-in-p & p-in-n) and annealing
- Question: is this valid for p+ isolation technique in general?

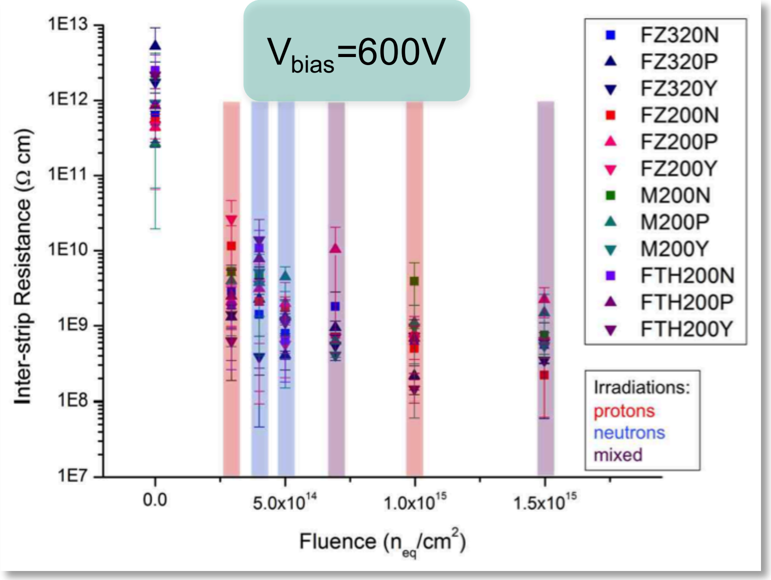

Results on R_{int} measurements

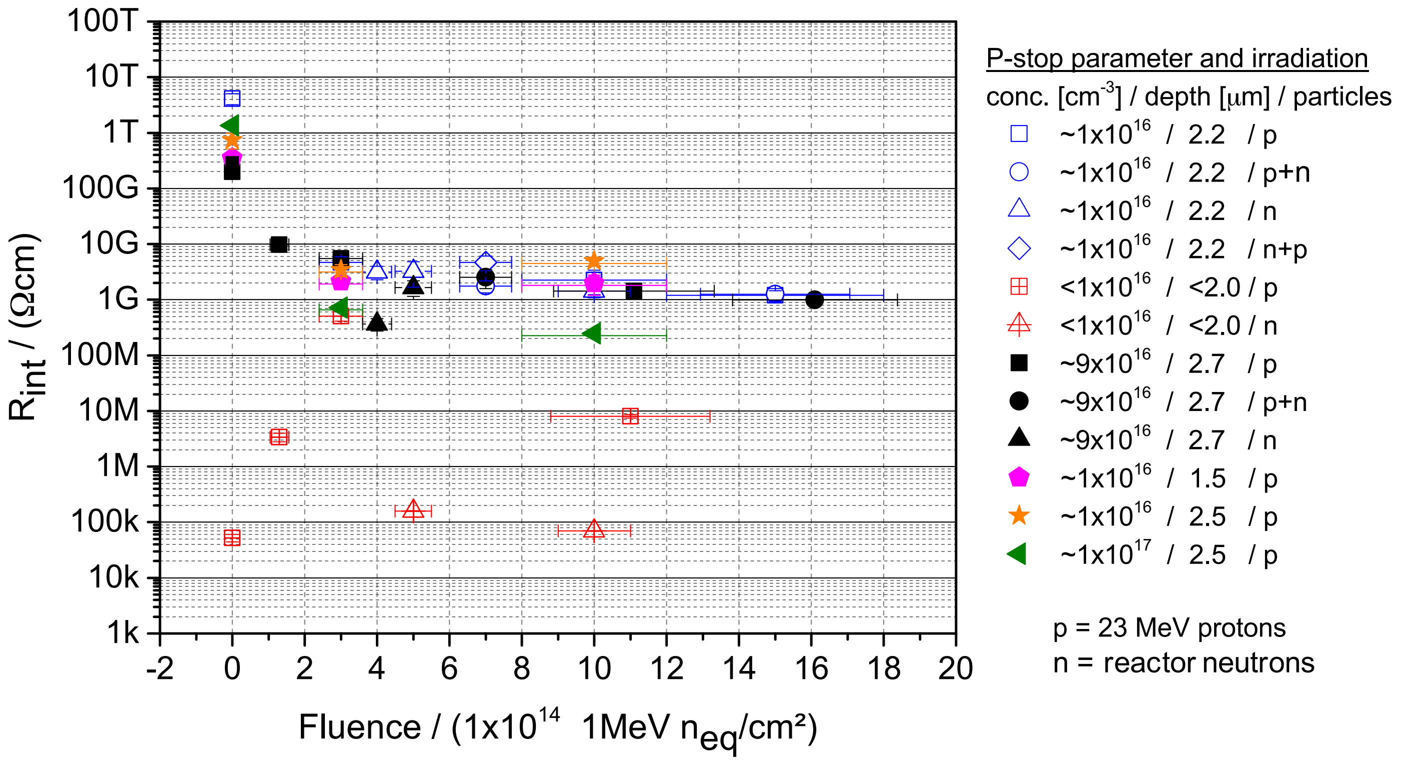

- R_{int} drops after irradiation by about three orders of magnitude but is **still high enough for good strip isolation** ($R_{int} > 20*R_{poly}$)
- <<$1x10^{16}cm^{-3}$ sensors show no strip isolation before irradiation -> P-stop conc. too low
  - After proton irradiation R_{int} increases

Sr90 measurement with ALiBaVa setup

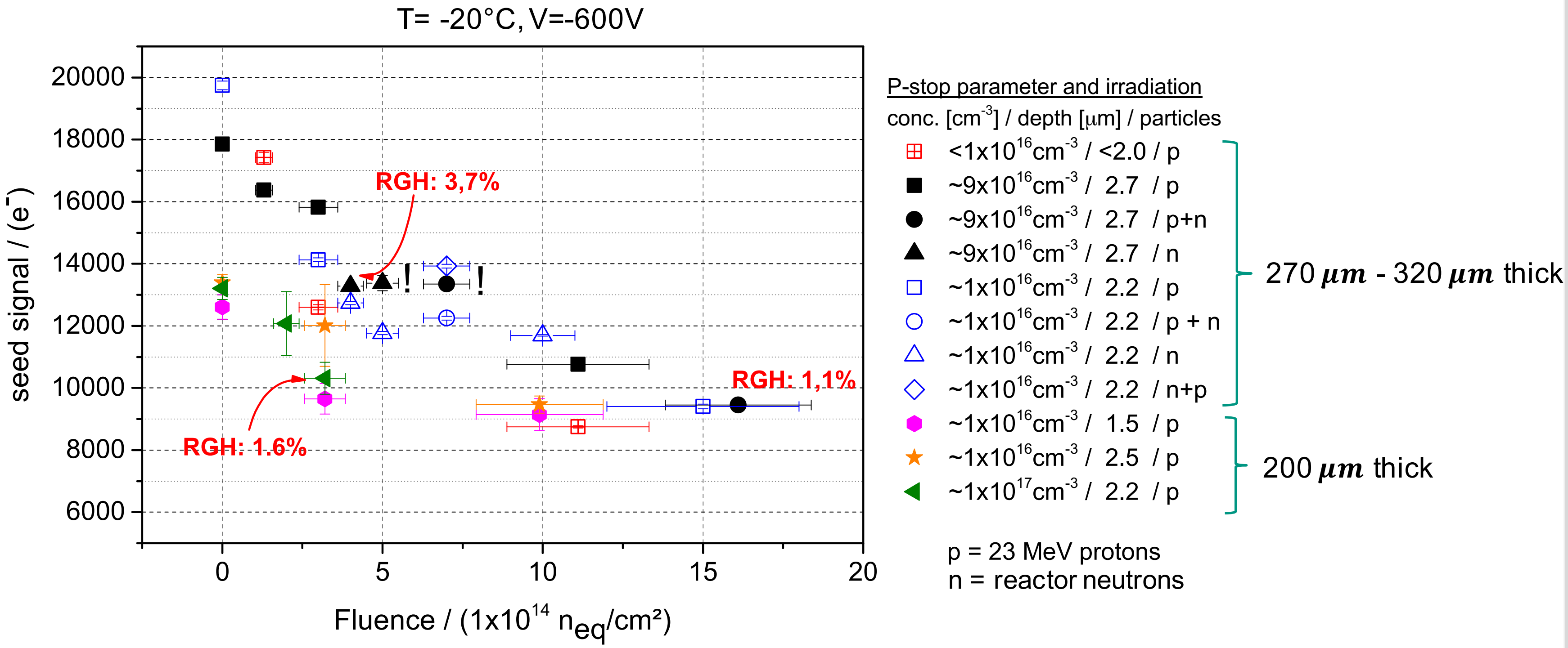

- CC is comparable for all vendors
- $<1\times10^{16}$ cm^{-3} sensors can be measured after proton irrad. due to increased R_{int} (positive space charge effect)
- 9×10^{16} cm^{-3} and 1×10^{17} cm^{-3} sensors show random ghost hits (!) after neutron, proton or mixed irradiation
  - T-CAD studies show that additional oxide charge lowers max. electric fields in n-in-p type sensors
- **1×10^{16} cm^{-3} sensors and 1.5 µm, 2.2 µm and 2.5 µm show no critical behaviour**

Noise contribution

- Non-gaussian noise/ Random Ghost Hits RGH mainly on p-in-n type sensors irradiated with charged hadrons
  - Random ghost hits (RGH): number of hits per strip and event above 5σ of gaussian fit divided by #strips and #events in a pedestal run without source
  - A number above 1% was defined as bad, since this would generate 1% occupancy with fakes
  - fake hits equally distributed over all strips
  - large RGH phase space for p-in-n type
  - P-type sensors with moderate p-stop conc. (~1x10^{16}cm^{-3}) almost not affected

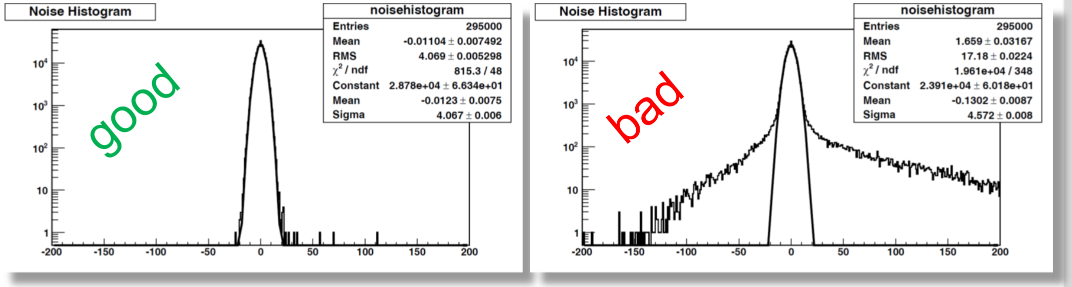

Fig.: Noise histogram from pedestal runs; left good, right non-gaussian!

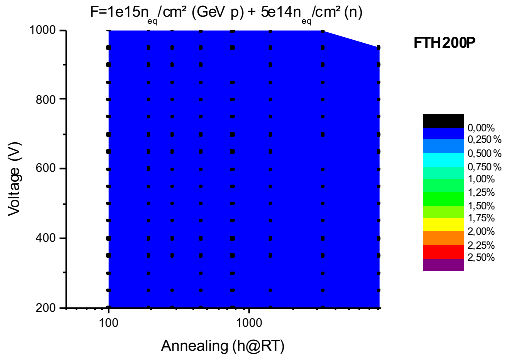

Fig: RGH in n-in-p type

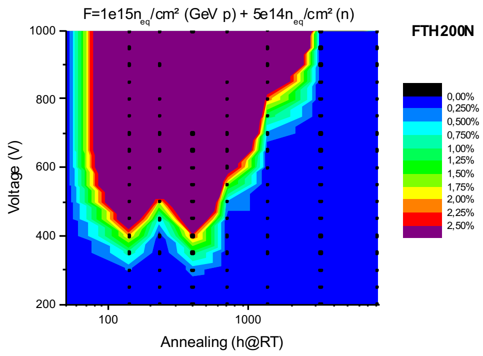

Fig: RGH in p-in-n type

P-stop concentration

- P-stop concentration singnifincantly influences the noise contribution

P-stop conc.= $9\mathrm{x}10^{16}\ \mathrm{cm}^{-3}$

$\Phi=1.6\mathrm{x}10^{15}\ n_{eq}/cm^2$, -900V

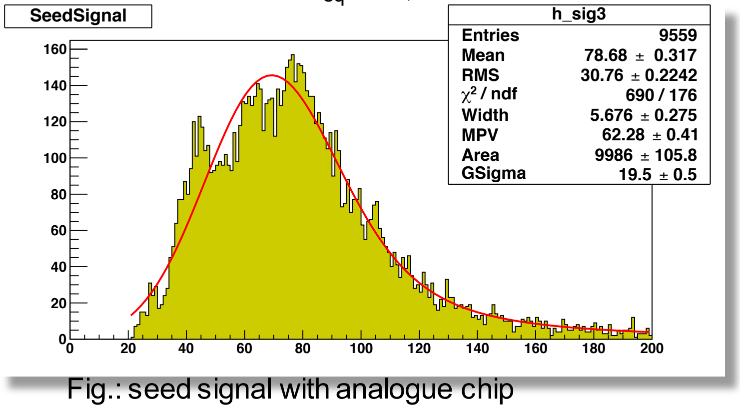

P-stop conc.= $1\mathrm{x}10^{16}\ \mathrm{cm}^{-3}$

$\Phi=2.0\mathrm{x}10^{15}\ n_{eq}/cm^2$, -900V

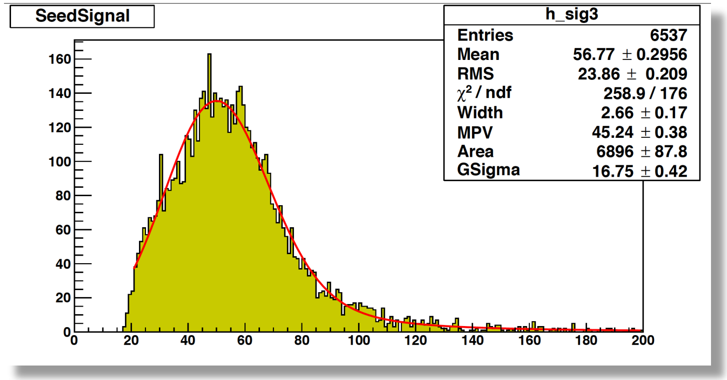

Fig.: seed signal with analogue chip

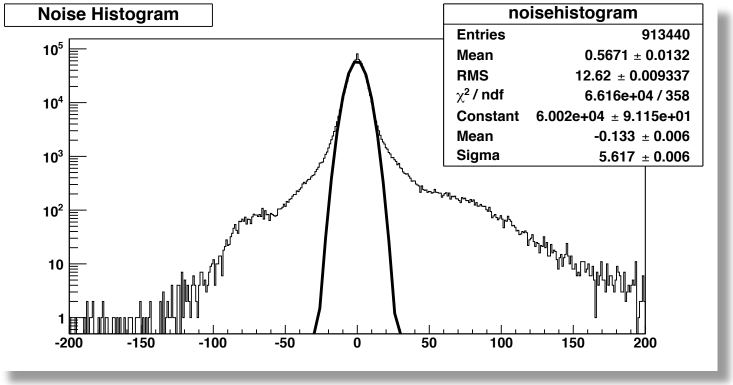

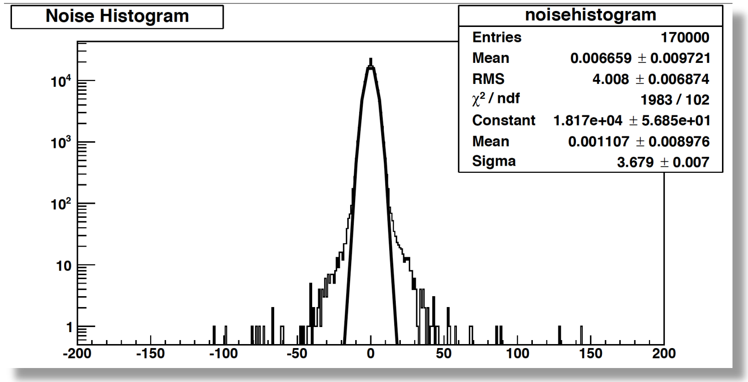

Fig.: pedestal run with random trigger

P-stop conc. $\geq 9\text{x}10^{16}$ cm^{-3}

- High p-stop concentration ~$9\text{x}10^{16}$ cm^{-3} and ~$1\text{x}10^{17}$ cm^{-3}
  - strip isolation is given even after very high fluence
  - but more and more non-gaussian noise appears with fluence, especially after neutron irradiation

$\Phi=1.6\text{x}10^{15}$ n_{eq}/cm^2, -900V

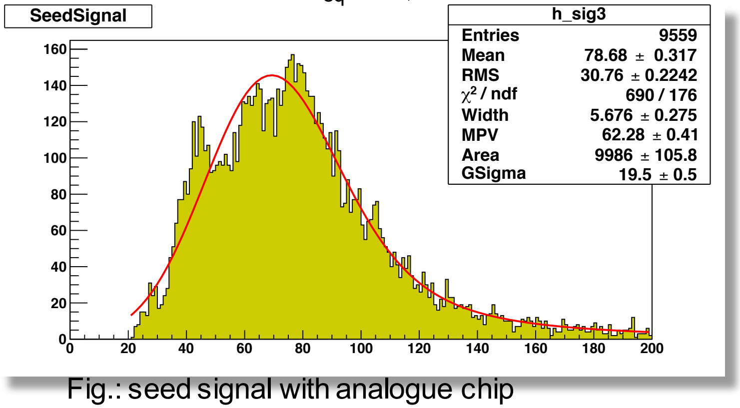

Fig.: seed signal with analogue chip

T-CAD: -900V, T=-20°C

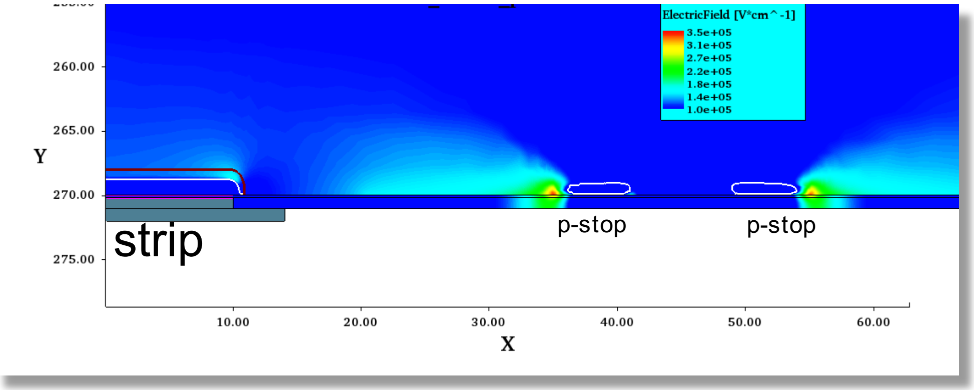

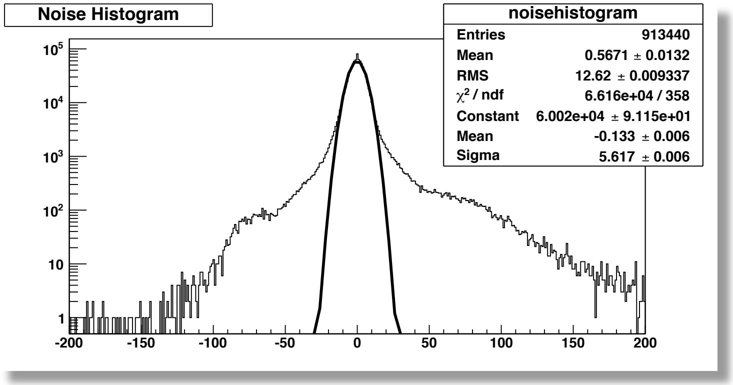

Fig.: pedestal run with random trigger

- RGH occur just for sensors with high p-stop conc. (V2&V4)
- locally very high electric fields (>30kV/cm) near p-stop
- P-stop conc. >$9\text{x}10^{16}$ cm^{-3} seems to be too high
  - Good R_{int} before and after irradiation
  - High random ghost hit rate (>1% after $4\text{x}10^{14}$ n_{eq}cm^{-2} neutrons)

T-CAD studies on electric fields: p-stop concentration

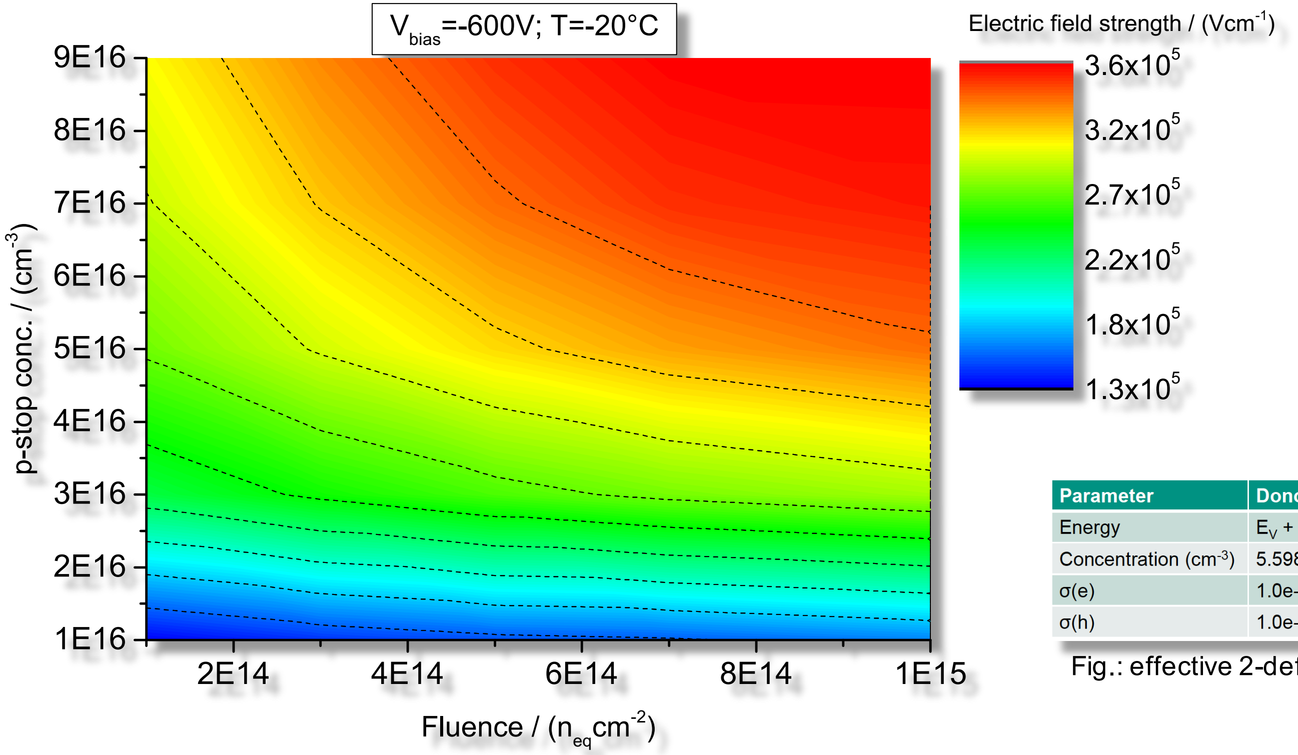

Parameter	Donor	Acceptor
Energy	E_V + 0.48eV	E_C - 0.525eV
Concentration (cm^{-3})	5.598 * F – 0.959e14	1.189 * F + 0.645e14
σ(e)	1.0e-14cm^2	1.0e-14cm^2
σ(h)	1.0e-14cm^2	1.0e-14cm^2

Fig.: effective 2-defect proton model

- Scan of the electric field with T-CAD Sentaurus in dependence of the Fluence and p-stop doping concentration
- Two-defect proton model (Eber, Phd 2013) used
- (Sensor parameter for simulation: bulk doping 1x10^{12} cm^{-3}, n+ implant 1x10^{19} cm^{-3} (gaussian) and 1.5 μm deep, backside doping 5x10^{18} cm^{-3} (erf), strip pitch 90 μm, strip width 25 μm, MetalOverhang 6 μm, N_{Ox}=1x10^{12} cm^{-2}, P-stop strip disctance PS=25 μm)
- **Developed model on data from measurements predicts high electric field strength and low breakdown voltage with increasing p-stop doping concentration**

T-CAD studies on electric fields: p-stop to strip distance

P-stop conc. = 9×10^{16} cm^{-3}, V = -600 V, T = -20 °C

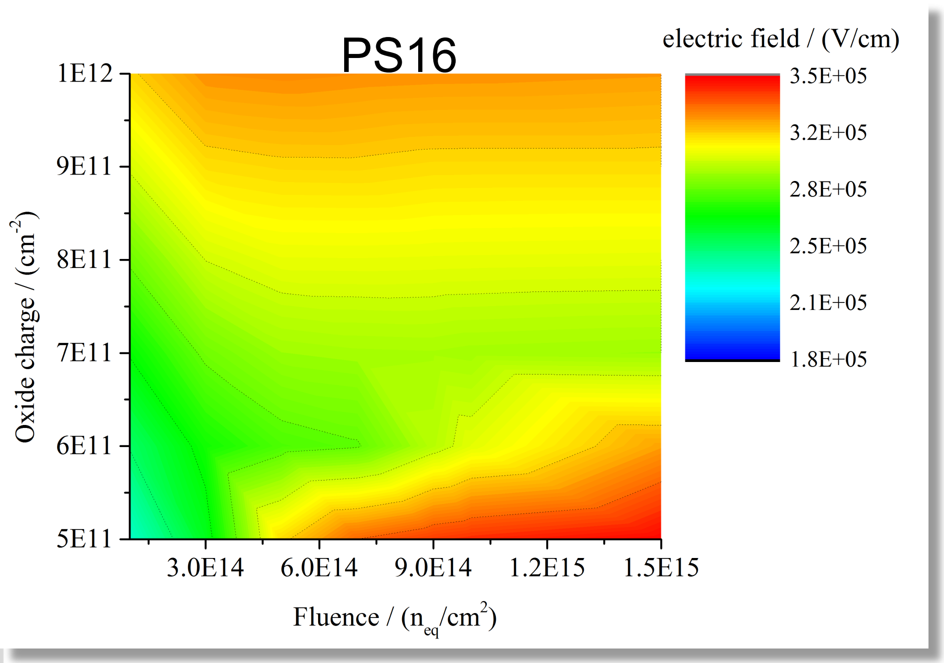

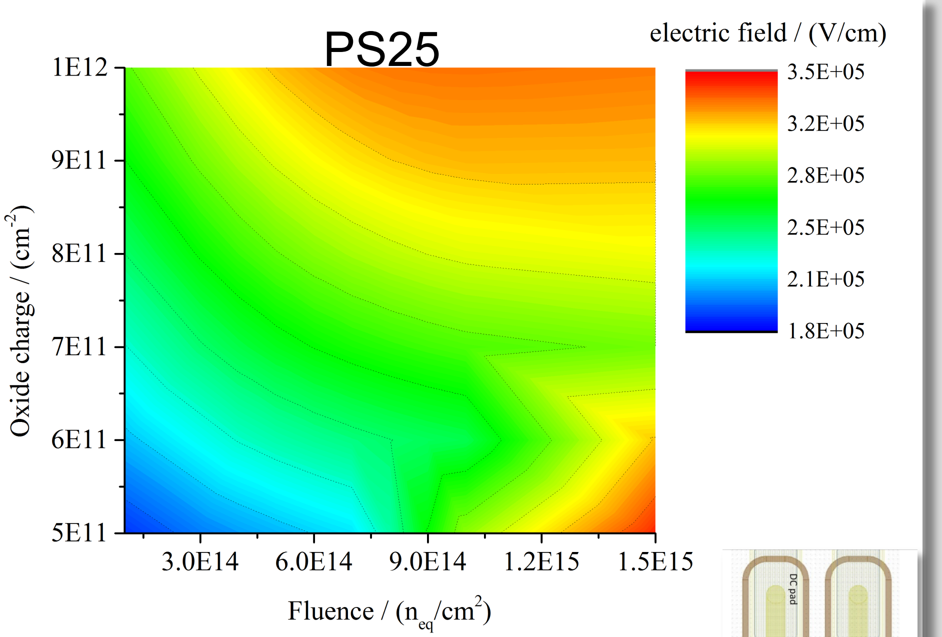

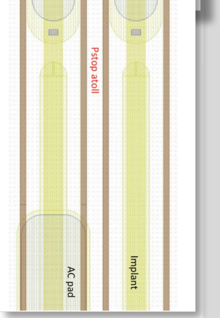

- Scanned the electric field in dependence on fluence and N_{ox} for p-stop conc. ~9×10^{16} cm^{-3}
- Very high electric fields at the p-stops are observed which induce avalanche effects -> RGH
- P-stops placed near the n+ strips lead to higher electric field strength at lower irradiation level and lower brakedown voltage

T-CAD studies on electric fields: implantation depths

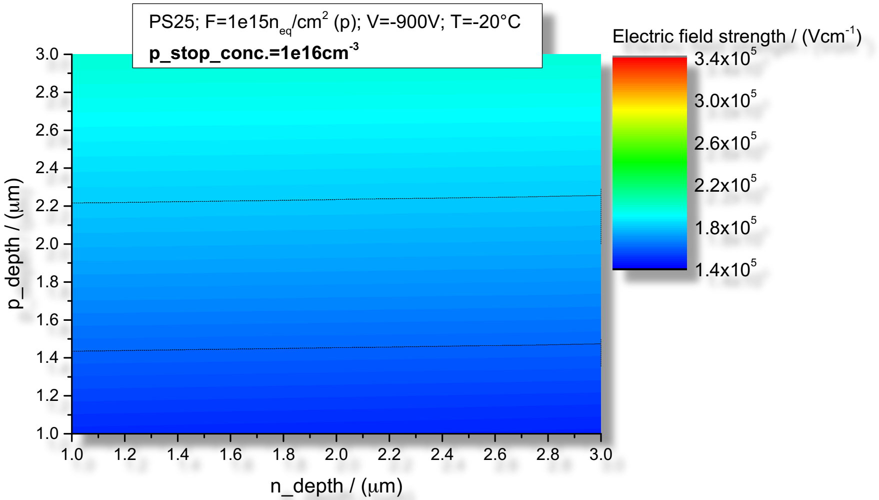

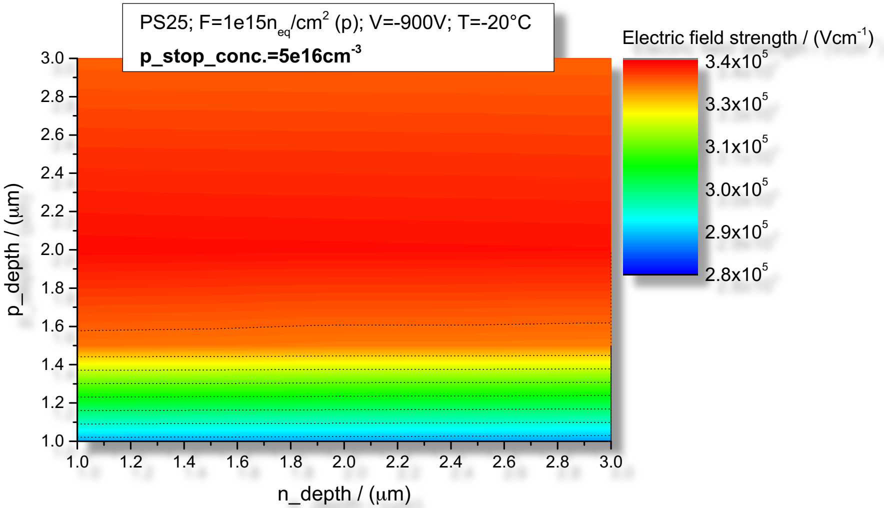

- Two-defect model used
- Extracted maximum electric field strength from the simulation
- Scanned the doping depths of n+ and p+ implants
    - Electric field strength is not dependent on the depth of n+ implants
    - P-stop depth significantly affects the electric field strength if concentration high

P-stop atoll pattern

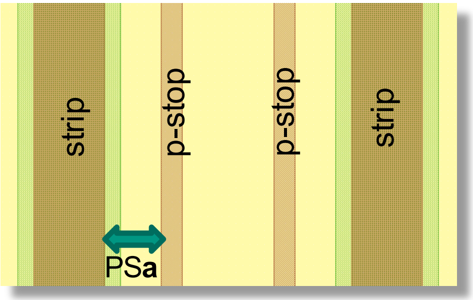

Fig.: from GDS file

- **PSa**= distance between strip and p-stop in µm
- **Electrical qualification**
  - no difference before and after irradiation
    - IV, CV, R_{int}, C_{int}

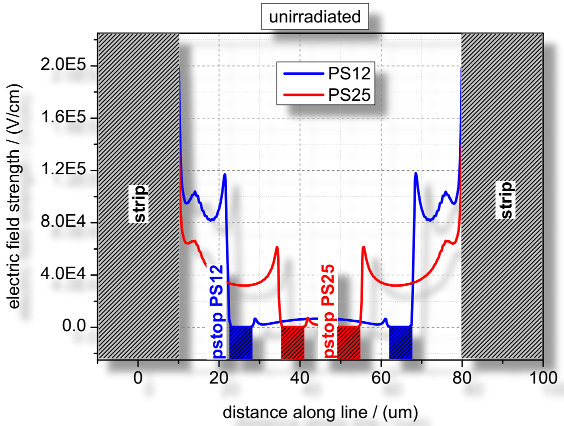

Fig.: T-CAD simulation of electric field

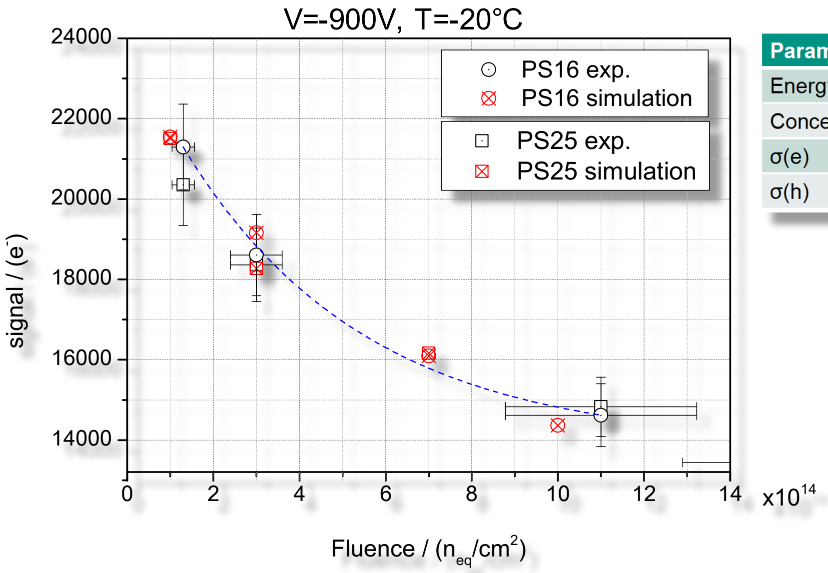

Parameter	Donor	Acceptor
Energy	E_V + 0.48eV	E_C - 0.525eV
Concentration (cm^{-3})	5.598 * F – 0.959e14	1.189 * F + 0.645e14
σ(e)	1.0e-14cm^2	1.0e-14cm^2
σ(h)	1.0e-14cm^2	1.0e-14cm^2

- sensors have been irradiated with 23MeV p and 1MeV n up to $\Phi=1.6\times10^{15}$ 1MeV n_{eq}/cm^2
- Sr90 measurements with fast readout system (ALiBaVa)
- **CCE measurements of irradiated samples reproduce predictions from simulations**
- **no significant difference of CCE in ALiBaVa depending on p-stop atoll pattern**

Interstrip measurements – cosmic telescope

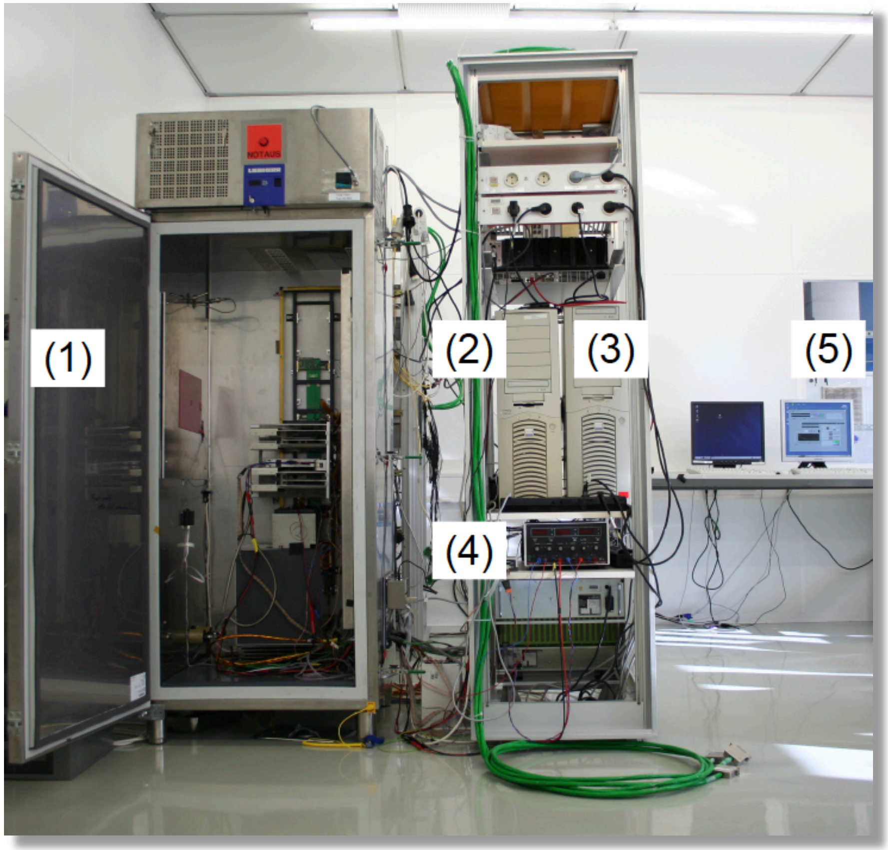

Fig.: Cosmic telescope at KIT
- (1) fridge
- (2) DAQ PC
- (3) SlowControl PC
- (4) LV Supply
- (5) monitoring

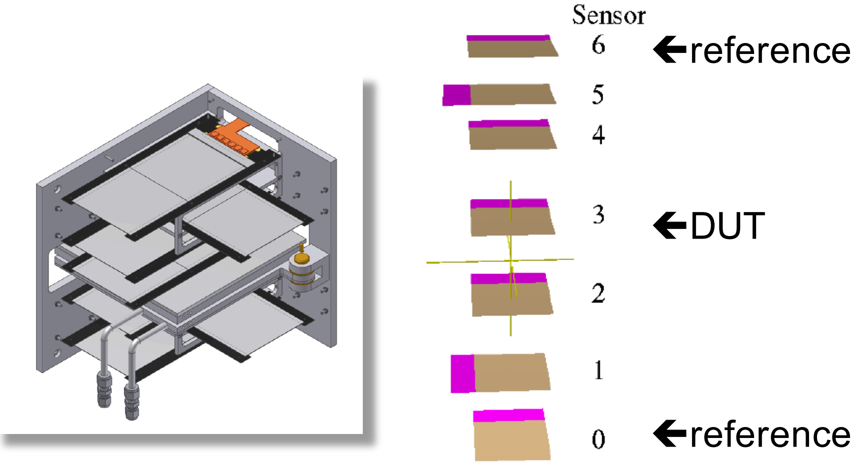

Fig.: CAD drawing of the telscope planes

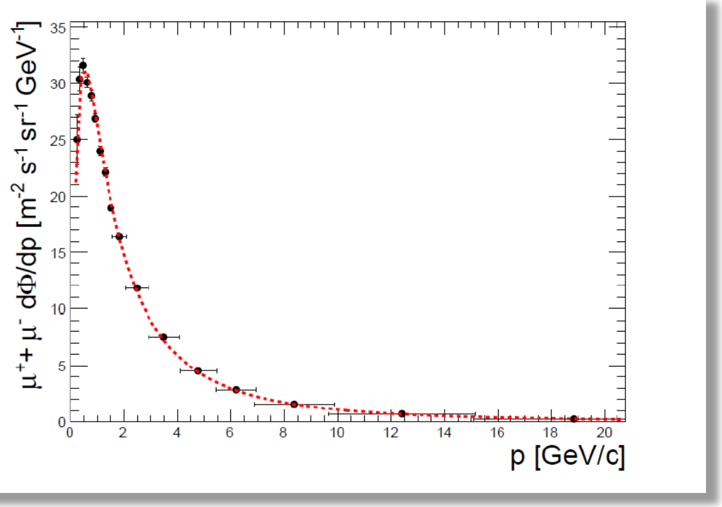

Fig.: differentail flux of cosmic myons at sea level

Results

unirradiated

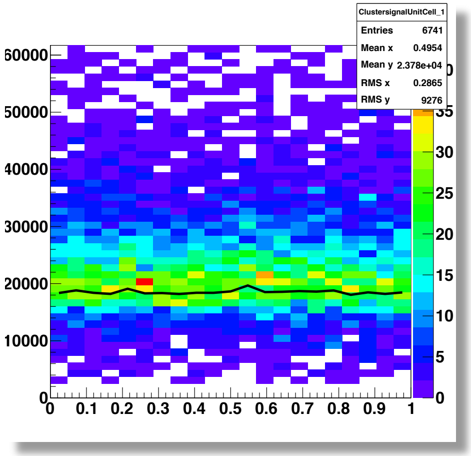

PS16 cluster signal unirr

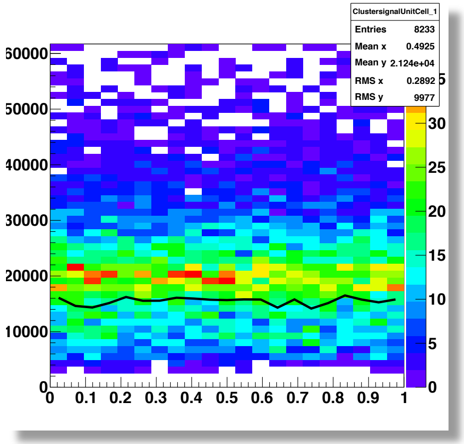

PS25 cluster signal unirr

Proton, F=1x10^{14} $n_{eq}cm^{-2}$

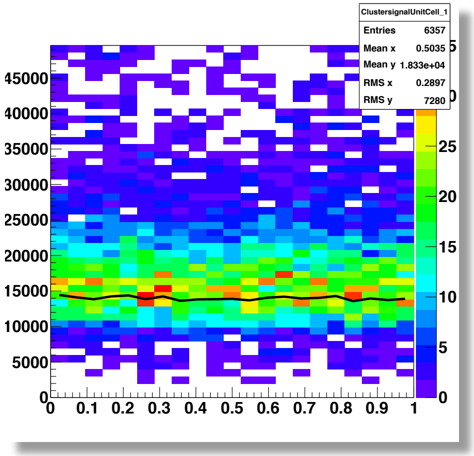

PS16 cluster signal 1e14p

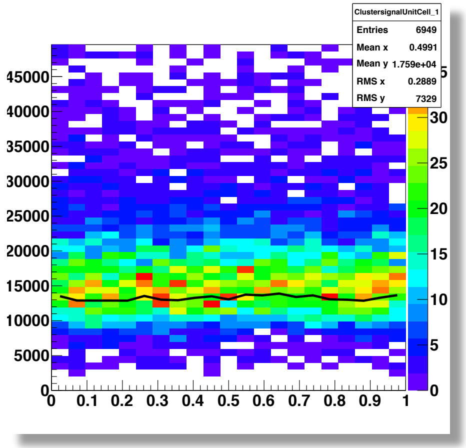

PS25 cluster signal 1e14p

- Unit cell:
  - x=0.5=center of strip
  - x=0&x=1 center of two adjacent strips
- Each vertical bin contains a charge distribution, which has been fitted with a convoluted landau and Gaussian function
- black line represents the most probable value of the fit in each bin
- No significant difference in signal depending on the p-stop atoll pattern
- Validates the Sr90 measurements
- (More statistics during next beam test)

Sum up

- CMS tracker collaboration studies n-in-p type sensors with p-stops in detail
    - Tools: T-CAD, Sr90 measurements, telescope, beam test
    - P-spray as alternative will be investigated in more detail now with new batches

- phase space for initial p-stop doping concentration can be reduced step by step
    - $<1\times10^{16}$ cm^{-3} too low
    - 9×10^{16} cm^{-3} seems to be too high
    - 1×10^{16} cm^{-3} with a doping depth of around 2 µm seems robust up to $\Phi=2\times10^{15}\ n_{eq}cm^{-2}$
        - to be confirmed with 6 new batches from 3 different vendors

- Simulation models have been developed and „confirmed“ by measurements of new sensors

- p-stop atoll pattern: p-stop to strip distance can be varied between 15 µm and 25 µm without changes in performance up to $\Phi=2\times10^{15}\ n_{eq}cm^{-2}$
    - Telescope measurements so far up to $\Phi=1\times10^{14}\ n_{eq}cm^{-2}$

backup

neutron model

Parameter	Donor	Acceptor
Energy (eV)	$E_V + 0.48$	$E_C - 0.525$
Concentration (cm^{-3})	1.395 cm^{-1} x F	1.55 cm^{-1} x F
σ(e) (cm^2)	1.2×10^{-14}	1.2×10^{-14}
σ(h) (cm^2)	1.2×10^{-14}	1.2×10^{-14}

proton model

Parameter	Donor	Acceptor
Energy (eV)	$E_V + 0.48$	$E_C - 0.525$
Concentration (cm^{-3})	5.598 cm^{-1} x F – $3.949 \cdot 10^{14}$	1.189 cm^{-1} x F – $6.454 \cdot 10^{13}$
σ(e) (cm^2)	1.0×10^{-14}	1.0×10^{-14}
σ(h) (cm^2)	1.0×10^{-14}	1.0×10^{-14}

- Synopsys Sentaurus TCAD sw package
- developed effective 2-trap model (R. Eber, Phd Thesis, IEKP-KA/2013-27, KIT) in order to simulate irradiated silicon sensors
- tables show models for neutron and proton irradiation
- developed on data from HPK silicon sensor for the PhaseII Outer Tracker campaign

- message:
  - models tuned in order to reproduce data from lab measurements (full depletion voltage, leakage current, charge collection and TCT)
  - can be used to investigate new silicon sensor characteristics and CCE

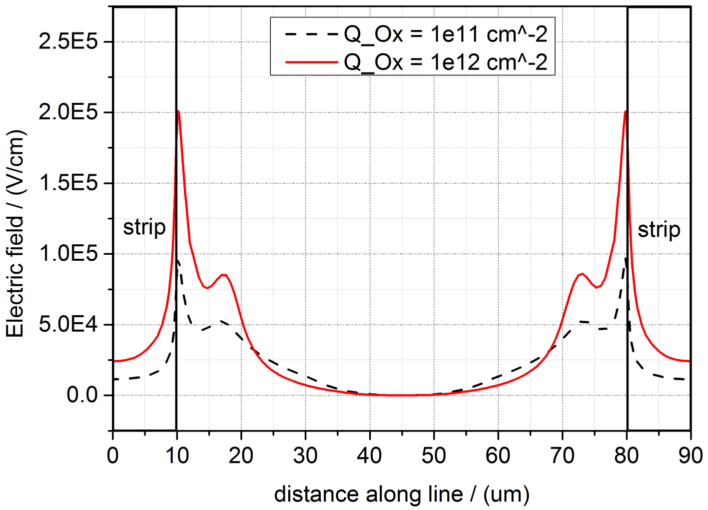

p-in-n type

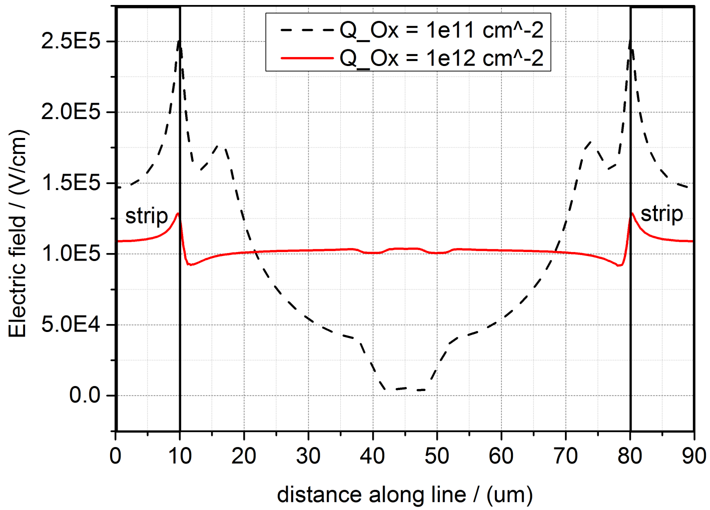

n-in-p type
with atoll p-stop isolation

- Synopsys Sentaurus T-CAD simulation of silicon strip sensors
- electric field strength for both polarities
- pitch and w/p are chosen corresponding to the Tracker Phase II Upgrade baseline with 2S modules
- simulated at V_{bias}=-1000V and T=-20°C
- cut through electric field 1.3µm below silicon/SiO_2 interface (p-n junction of bulk and strip implant)
- 2-trap proton model applied: $F=1x10^{15}\ n_{eq}/cm^2$

- message:
  - ionizing radiation introduces positive oxide charge Q_{Ox} (saturation of Q_{Ox} expected to be ~$1e12cm^{-2}$)
  - increasing Q_{Ox} decreases the electric field strength in n-in-p devices → less prone to micro-discharges/break through

Electric field strength: F vs. N_{Ox}

- scanned fluence from 1e14 to 1.5e15 n_{eq}/cm^2 (20 cm)
  - two-defect proton model (Phd Robert)
- scanned oxide charge from 5e11 to 1e12 cm^{-2} (XFEL study, Zhang)
  - surface defects still not implemented sufficiently

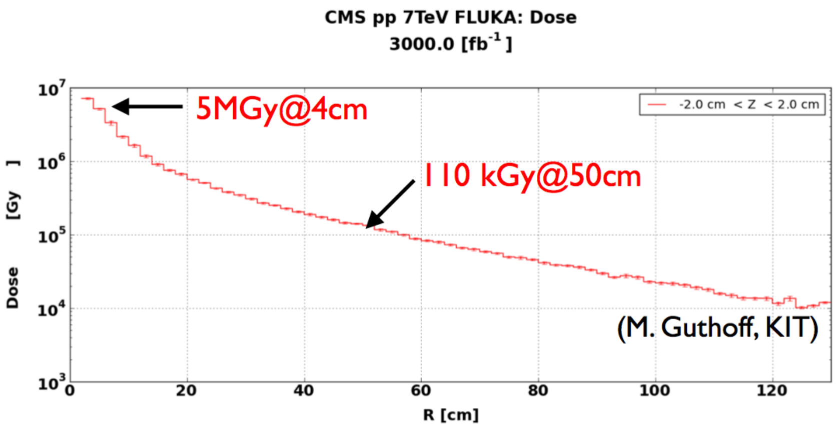

5MGy@4cm

110 kGy@50cm

(M. Guthoff, KIT)

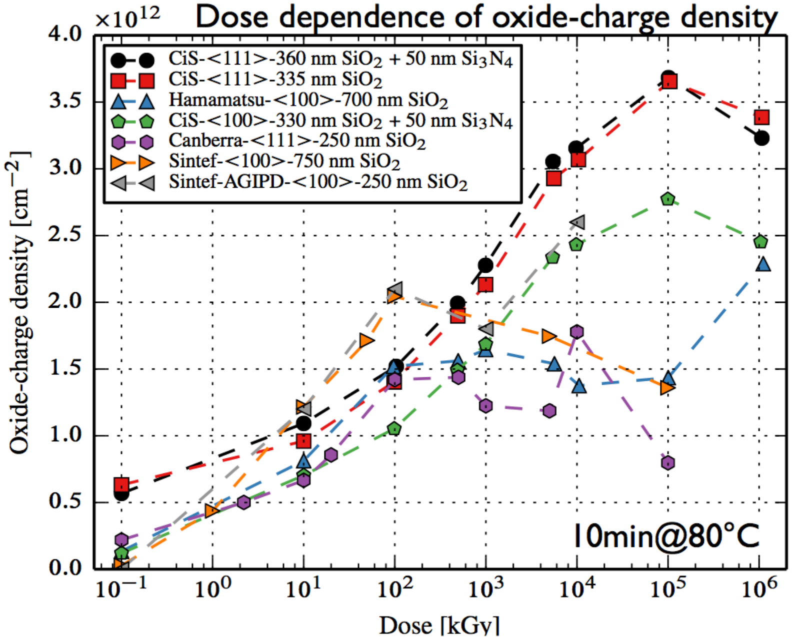

10min@80°C

- how does surface damage influence overall performance after high radiation dosis?

Backup

2S-module

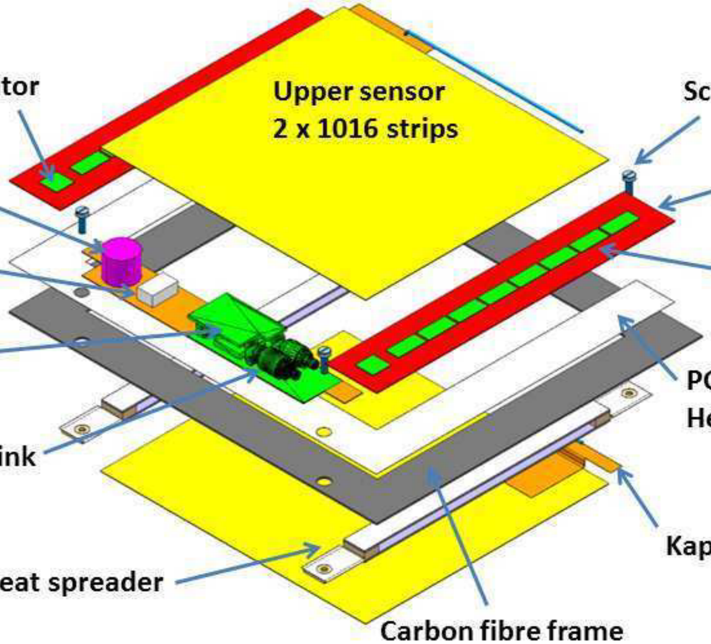

Concentrator

DC-DC converter

Connector

GBT

Optical link

Heat spreader

Carbon fibre frame

Kapton insula

PGS foil to augment
Heat conductance

CBC

Hybrid

Screws

Upper sensor
2 x 1016 strips

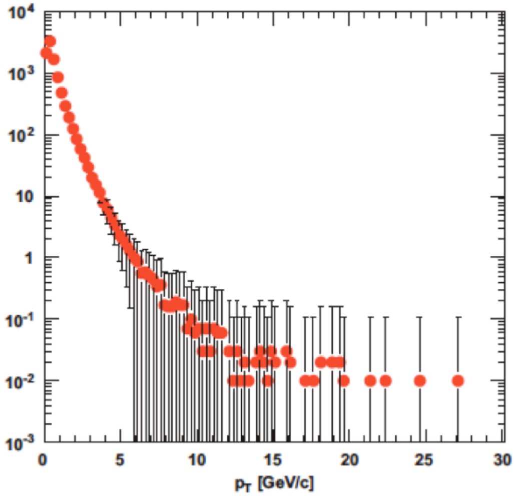

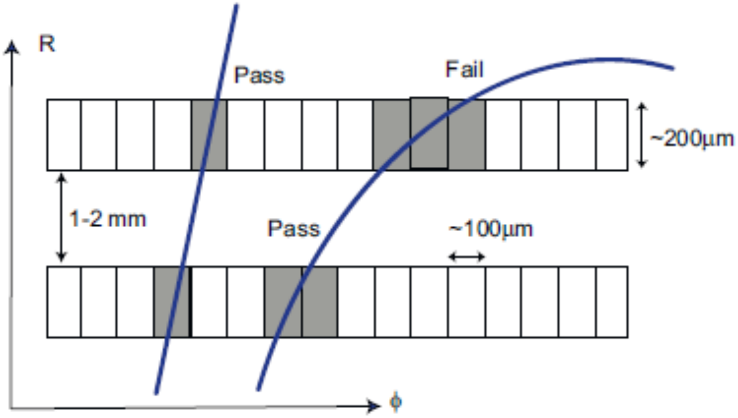

Temperature Dependence of RGHs

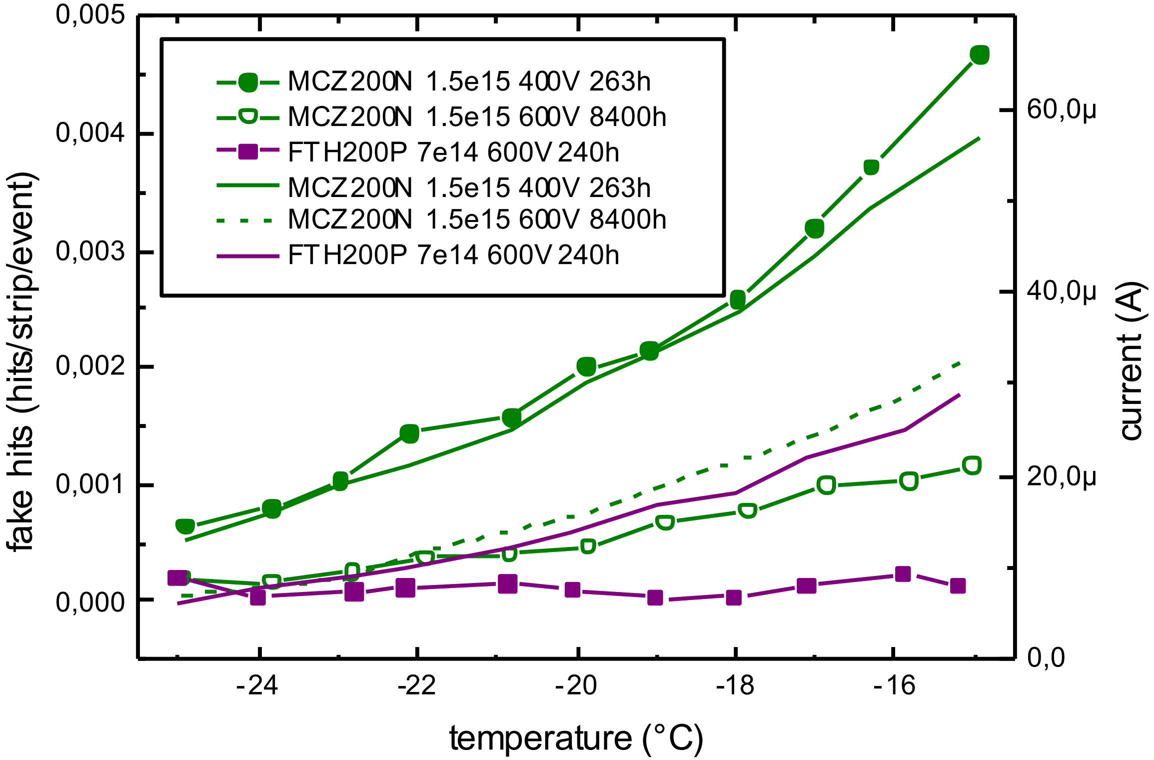

- Fake hit rate increases with temperature following current!
- The increase of fake hit rate is typically linked to an increase in current. But an increase in current does not necessarily lead to fake hits.